J. Fluid Mech. (1988), *vol.* 188, *pp.* 23–45
Printed in Great Britain

The nature of upstream blocking in uniformly stratified flow over long obstacles

By PETER G. BAINES AND FIONA GUEST
CSIRO Division of Atmospheric Research, Aspendale, Victoria 3195, Australia

(Received 27 September 1986 and in revised form 25 May 1987)

The general method described in Baines 1988 has been applied to stratified flows of finite depth over long obstacles where the flow initially has uniform horizontal velocity. The fluid consists of a finite number of homogeneous layers of equal thickness and with equal density increments. This represents the state of continuous stratification with constant density gradient as closely as possible, for a given number of layers. Two-, three-, four- and sixty-four-layered models are studied in detail. The results are expressed in terms of the initial Froude number F_0 ($F_0 = U/\hat{c}_1$ where U is the fluid speed and $\hat{c}_1$ is the speed of the fastest long internal wave mode in the fluid at rest) and the obstacle height. In general, introduction of an obstacle into the flow causes disturbances to propagate upstream (columnar disturbance modes) which alter the velocity and density profiles there. These may accumulate to cause upstream blocking of some of the fluid layers if F_0 is sufficiently small. As the number of fluid layers increases, so does the range of F_0 for which this upstream blocked flow occurs. There are no upstream disturbances for $F_0 > 1$, and for $F_0 < 1$ the upstream disturbances are of the rarefaction type if upstream blocking does not occur. The results for three and four layers show how several coexisting modes may interact to affect the upstream profiles. The results for sixty-four-layers provide theoretical support for the observational criterion (Baines 1979*b*) that blocking in initially uniformly stratified flow occurs when $Nh_m/U > 2$ (N is the Brunt–Väisälä frequency and h_m the obstacle height), provided that more than two modes are present. In some situations, layered models are found to be inadequate as a representation of continuous stratification when one or more layers thicken to the extent that their discreteness is significant.

1. Introduction

A general method for determining the properties of stratified flow upstream and over long two-dimensional obstacles for quite general finite-depth flows has been described by Baines (1988, hereinafter referred to as I). The procedure depends on representing the fluid by a number of homogeneous layers. In this paper the method is applied to fluids which initially have uniform horizontal velocity, and in which the homogeneous layers all have equal thicknesses and density increments. This is as good an approximation to a uniformly stratified fluid as can be achieved with a given finite number of layers. Upper and lower horizontal boundaries are assumed to be rigid, and the volume flux is an invariant of the system. Two-, three-, four- and sixty-four-layered systems are studied in detail. In all cases the overall density variation is taken to be small, although the model does not require this.

It is known from laboratory observations that the introduction of an obstacle into a stratified flow causes upstream disturbances which alter the approaching upstream

flow. The situation for two-layer systems has been discussed in detail in Baines (1984) for a wide range of values of the ratio of the layer thickness. The contrasting case of uniform stratification has also been much studied theoretically because it represents the other extreme. Apart from the linear perturbation solutions for obstacles of small height, there are the steady-state solutions for obstacles of finite height obtained by Long (1955), using equations in a form generally known as Long's model, and the nonlinear perturbation study by McIntyre (1972). The Long's model solutions are only obtainable in the case of uniform stratification (or more precisely, when the vertical profile of kinetic energy $\frac{1}{2}\rho U^2$ is constant with height), and may be regarded as an extension to finite obstacle height of the linear solutions, which they closely resemble. The calculation by McIntyre was stimulating in that, as a formal perturbation expansion in the obstacle height, it revealed no upstream disturbances at all other than very weak ones generated in the tails of the lee waves. Subsequent laboratory experiments (Wei, Kao & Pao 1975; Baines 1977, 1979*a*) have shown that the upstream disturbances observed are much stronger and are generated by nonlinear effects in the flow above the obstacle. These disturbances may be generated for quite small obstacle heights provided that the flow conditions are close to resonance for a long internal wave mode (on the subcritical side of resonance for uniform stratification), and the occurrence and magnitude of the effects are observed to increase with increasing obstacle height. Furthermore, the disturbances may accumulate to result in upstream blocking of low-level fluid. The mathematical situation has recently been clarified in two studies by Grimshaw & Smyth (1986) and Melville & Helfrich (1987), who have shown that, for fairly long obstacles of small height near resonance, the upstream disturbances and their generation may be described by equations of the forced Korteweg–de Vries type.

The present study may be seen as being complementary to those of Grimshaw & Smyth and Melville & Helfrich because, whilst theirs is restricted to small obstacles and is not necessarily hydrostatic, the present work is necessarily hydrostatic but is not restricted in the height of the obstacle. The primary objective here has been to obtain an overall picture of the character of the flow upstream and over the obstacle in terms of the initial Froude number $F_0 = U/\hat{c}_1$ (where U is the initial fluid speed relative to the obstacle and $\hat{c}_1$ is the speed of the fastest internal wave mode in the fluid at rest) and $H = h_m/D$, where h_m is the maximum height of the obstacle and D is the total depth. The two-, three- and four-layer systems are described for the whole range of these parameters, and the sixty-four-layer system up to the point of blocking of the lowest layer for $F_0 > 0.2$.

The plan of the paper is as follows. The linear solutions and the corresponding Long's model solutions for hydrostatic flow are described in §2. The Long's model solutions for sufficiently large obstacle height, when valid, contain closed stagnant regions (or rather, recirculating regions which may be interpreted as stagnant). Solutions with such closed regions differ from those obtained with the layered models utilized in this paper, and the reasons for this difference are discussed. The detailed properties of the solutions for two, three and four layers are described in §3. The results for the sixty-four-layer model are given in §4, together with a discussion of the extent to which sixty-four-layers provide a good approximation to continuous stratification. The detailed characteristics of upstream blocking in these layered systems are described in §5, and the results are summarized in §6.

2. Linear solutions for small obstacles

We consider fluid of constant Brunt–Väisälä frequency N in a horizontal channel of depth D with rigid upper and lower boundaries. The total density variation $\Delta\rho$ is assumed to be small so that $\Delta\rho/\bar{\rho} \ll 1$, where $\bar{\rho}$ is the mean density. The channel contains bottom topography $z = h(x)$ where x is the horizontal and z the vertical coordinate; the topographic height is small, in that $h_m/D \ll 1$, and varies slowly in the horizontal, so that $dh/dx = O(h_m/a)$ where $2a$ is the obstacle length and $D/a \ll 1$. The equations governing disturbances to uniform flow in the channel are then linear and hydrostatic. If the flow has mean velocity U with perturbation (u, w) given by

$$u = -\frac{\partial\psi}{\partial z}, \quad w = \frac{\partial\psi}{\partial x}, \tag{2.1}$$

the disturbance streamfunction ψ is governed by

$$\left(\frac{\partial}{\partial t}+U\frac{\partial}{\partial x}\right)^2\frac{\partial^2\psi}{\partial z^2}+N^2\frac{\partial^2\psi}{\partial x^2}=0, \tag{2.2}$$

with

$$\left.\begin{aligned}\psi &= Uh(x) \quad (z=0),\\ &= 0 \quad\quad (z=D).\end{aligned}\right\} \tag{2.3}$$

If the mean motion is started impulsively at $t = 0$, the initial conditions are

$$\psi = \psi_P = Uh(x)\left(1-\frac{z}{D}\right) \quad (t=0), \tag{2.4}$$

where ψ_P denotes potential flow, and

$$\left(\frac{\partial}{\partial t}+U\frac{\partial}{\partial x}\right)\left(\frac{\partial^2\psi}{\partial z^2}\right)=0 \quad (t=0), \tag{2.5}$$

which implies initially horizontal density surfaces.

The complete solution of this initial-value problem is

$$\psi = Uh(x)\frac{\sin K\pi(1-z/D)}{\sin K\pi}$$
$$-U\frac{K}{\pi}\sum_{m=1}^{\infty}\left(\frac{h(x-(1-K/m)Ut)}{m-K}-\frac{h(x-(1+K/m)Ut)}{m+K}\right)\frac{\sin(m\pi z/D)}{m}, \tag{2.6}$$

provided that $K = ND/\pi U$ is not an integer ($K = 1/F_0$ for this system). This solution consists of a number of parts, each of which has the same horizontal structure as the obstacle, $h(x)$. The first term is the steady-state part of the solution, and the remaining terms consist of two 'transient' terms for each mode m, one propagating against the stream and one propagating with it; of these two the former has the larger amplitude. If the parameter $K = ND/\pi U$ lies in the range $n < K < n+1$ where n is any integer, modes 1 to n have propagation speeds $ND/n\pi$ greater than the fluid speed U, so that the left-ward propagating disturbance for these modes can move upstream relative to the obstacle. For modes $n+1, n+2, \ldots, \infty$, on the other hand, both disturbances are found downstream.

The interesting point about this simple solution is that it becomes singular as K approaches any integer n. Both the steady-state component and the larger-amplitude wave-component for mode n increase without limit, as $K \to n$, and the

propagation speed of the latter approaches zero. If $K = n$, the solution to the above initial-value problem has the form

$$\psi = \frac{U^2 t}{n\pi}\frac{dh}{dx}\sin\frac{n\pi z}{D} + Uh(x)\left[\left(1-\frac{z}{D}\right)\cos\frac{n\pi z}{D} - \frac{2}{n\pi}\sin\frac{n\pi z}{D}\right] + \frac{Uh(x-2Ut)}{2n\pi}\sin\frac{n\pi z}{D}$$
$$-\frac{UK}{\pi}\sum_{\substack{m=1\\ m\neq n}}^{\infty}\left(\frac{h(x-(1-K/m)Ut)}{m-K} - \frac{h(x-(1+K/m)Ut)}{m+K}\right)\frac{\sin(m\pi z/D)}{m}, \tag{2.7}$$

so that it grows linearly with time. This behaviour clearly implies that nonlinear factors must eventually become important when K is sufficiently close to an integer.

If the obstacle is semi-infinite in length with $h(x) \to$ constant as $x \to +\infty$, when $K > 1$ the upstream-propagating components also have infinite length, with the result that these 'transients' become permanent disturbances to the upstream flow. This linear upstream influence is well known (e.g. Wong & Kao 1970) and is purely an artefact of the semi-infinite obstacle. Its origin is quite different from that of the upstream disturbances for finite obstacles, with which this paper is mainly concerned.

The steady-state form of these solutions has been extended to obstacles of finite height by Long (1955), and the solution for the perturbation is

$$\psi = Uh(x)\frac{\sin K\pi(1-z/D)}{\sin K\pi(1-h(x)/D}. \tag{2.8}$$

The corresponding total density field then is

$$\frac{\rho}{\bar{\rho}} = 1 + \frac{\Delta\rho}{\bar{\rho}}\left(\frac{1}{2} - \frac{z}{D} + \frac{h\sin K\pi(1-z/D)}{D\sin K\pi(1-h/D)}\right). \tag{2.9}$$

Properties of this solution in terms of K and $H = h_m/D$ are represented in figure 1, for $h(x)$ both positive (obstacles) and negative (holes). If $|H|$ is small the solution is very similar to the linear steady-state solution, but as $|H|$ increases a value H_s is reached above which closed recirculating flow regions appear over the obstacle. Regions of figure 1 where this occurs are shaded, and two examples of such flows are shown in figure 2. As $|H|$ is increased above the value H_s, the closed recirculating regions in the solutions increase in thickness to fill the whole region of fluid above the obstacle crest, and the fluid velocity in the intervening gaps tends to infinity. The value of $|H|$ for which this occurs is denoted by H_∞, and the curves are given by

$$\sin K\pi(1-H_\infty) = 0. \tag{2.10}$$

When $|H| > H_\infty$ (in the stippled regions of figure 1) the Long's model solutions cannot represent possible flow fields.

The flow solutions with recirculating regions ($H_s < |H| < H_\infty$) contain fluid in these regions which is statically unstable. This implies that these solutions, taken literally, cannot represent real flows because such flows must be unstable. For the interior enclosed regions (such as in figure 2*b*) it is possible to interpret these solutions as representing flows with homogeneous stagnant fluid in the enclosed regions. This is because the solutions there are symmetric about the vertical, and the enclosed fluid may be replaced by a homogeneous fluid (with the local mean density) without changing the external pressure field. However, this is not possible for the regions attached to the upper boundary, as shown in figure 2(*a*). Hence this realistic interpretation of these solutions when $H_s < |H| < H_\infty$ is possible for K in the ranges

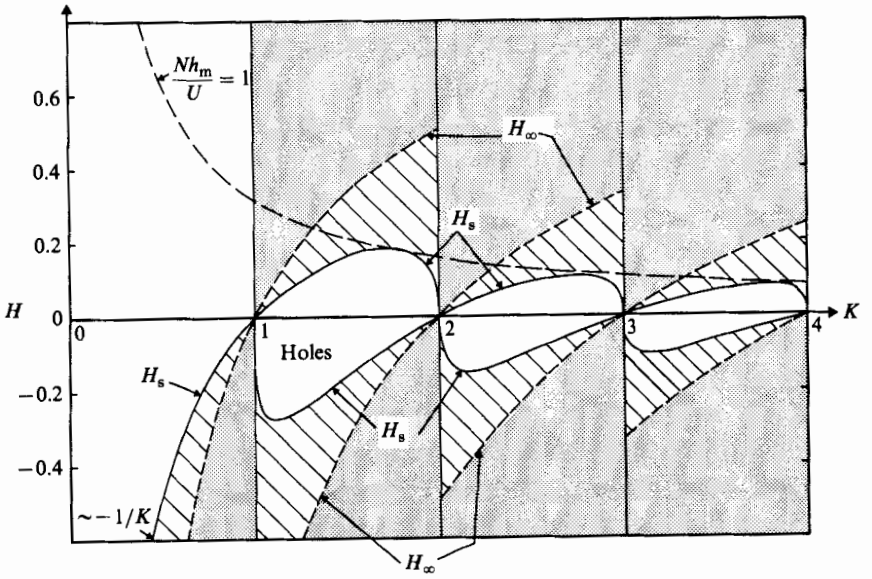

FIGURE 1. Properties of the hydrostatic Long's model solution in terms of $K = ND/\pi U$ and $H = h_m/D$. $H > 0$ corresponds to flow over obstacles, and $H < 0$ to flow over holes. In the clear regions the solution is statically stable; in the shaded regions ($H_s < |H| < H_\infty$) the solution contains closed recirculating regions, and in the stippled regions ($|H| > H_\infty$) the solutions cannot represent real fluid flows. The curve $Nh_m/U = 1$ is included for comparison.

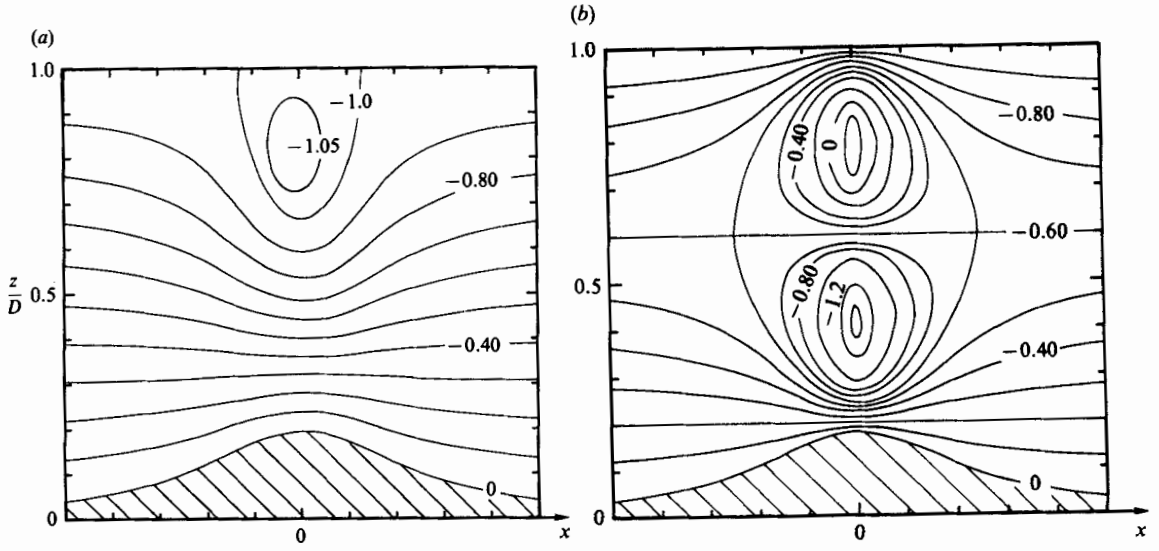

FIGURE 2. Two examples of Long's model solutions with closed regions, showing contours and values of the total streamfunction $(\psi - Uz)/UD$. These contours also denote streamlines and constant density surfaces. The shaded region at the bottom is the obstacle, $h(x)/D$. For hydrostatic flow, the horizontal scale is arbitrary. (*a*) $K = 1.5$, $h_m/D = 0.2$, (*b*) $K = 2.5$, $h_m/D = 0.18$.

$2 < K < 3$, $4 < K < 5$, etc. where all enclosed regions are internal, but is doubtful when $1 < K < 2$, $3 < K < 4$, etc.

The above discussion relates to hydrostatic flows over long obstacles. If the obstacle is not sufficiently long for the flow to be hydrostatic so that horizontal dispersion terms are not negligible (specifically, $\partial^2/\partial x^2 \sim \partial^2/\partial z^2$), the solution to the linear initial-value problem is more complicated but has the same general character. The steady-state solution is still singular at $K = n$, although the singularity is weaker, with $1/(K^2-n^2)^{\frac{1}{2}}$ behaviour, and it contains lee waves on the downstream side if $K > 1$. The two transient terms for each mode are still present and have 'tadpole-like' character, with decaying oscillatory tails. The time-dependent solution obtained when $K = n$ grows as $(Nt)^{\frac{1}{3}}$ rather than Nt, and hence nonlinear effects are expected here also. The Long's model solutions for short obstacles again have closed recirculating regions if $K > 1$ and the obstacle height is sufficiently large. The above remarks about interpreting the enclosed regions as containing stagnant homogeneous fluid are expected to be still applicable, although the picture is more complex because the recirculating flow in the enclosed regions in the solutions is not hydrostatic.

3. Nonlinear solutions for two, three and four layers

We now consider the application of the general procedure described in I to flows which consist of two, three or four homogeneous layers with equal density increments, and which, in the undisturbed state, have equal thickness and velocity. The flow resulting from the introduction of long obstacles of height h_m in a channel with a rigid upper boundary is characterized by two dimensionless parameters: $H = h_m/D$ where D is the channel depth, and a Froude number

$$F_0 = \frac{U}{U-c_1} = \frac{U}{-\hat{c}_1}, \tag{3.1}$$

where U is the initial fluid velocity and c_1 is the velocity (relative to the topography) of the fastest internal wave mode propagating against the stream. $\hat{c}_1 = c_1 - U$ is the wave speed in the same stratification when the fluid is at rest.

The procedure described in I involves the calculation of the steady-state flows over a succession of obstacles with steadily increasing height H, for a given value of F_0. The resulting solutions are described by specifying the properties of the velocity and density profiles immediately upstream. The procedure is repeated for a number of F_0 values, so that a complete description of the properties of the system may be given on a single diagram in the (F_0, H)-plane.

3.1. *Two layers*

The overall pattern of the results obtained from the model is shown in figure 3. These results may be derived independently by analytical methods. In particular, the curve for the onset of blocking of the lower layer is

$$F_0 = 2(2H-1)(1-H) \quad (0 < F_0 < 0.25), \tag{3.2}$$

and the depth of the blocked layer on this curve is equal to h_m.

The general response of the two-layer system to the introduction of an obstacle is as follows. When H is small, sudden commencement of motion yields two transient waves for the one internal wave mode, one propagating against the stream and one with it (as described for continuous stratification in the preceding section). If $F_0 > 1$ both of these are swept downstream, leaving steady flow which is everywhere

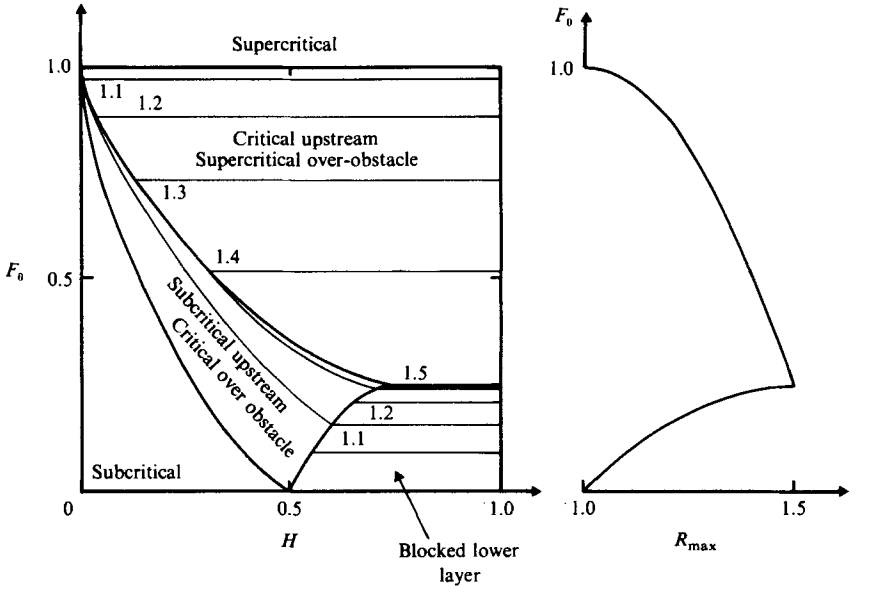

FIGURE 3. (F_0, H)-diagram for two equal layers, showing the amplitude of the upstream disturbance, and the regions where the lower layer is blocked or the upstream flow is critical (implying zero internal wave speed). The numbers give the values of R, the lower layer thickness relative to its undisturbed value. The maximum value of R, R_{max}, is shown on the right.

supercritical. This situation persists as H is increased up to its maximum value (unity); steady upstream and downstream flows are the same as in the initial state, and the only change is that the flow over the obstacle becomes more supercritical as H increases. If $F_0 < 1$, one transient wave propagates upstream and the other downstream, leaving subcritical flow over the obstacle. As H increases a point is reached where the flow becomes locally critical at the obstacle crest (i.e. locally, a linear wave speed is zero); a further increase in obstacle height then results in columnar disturbances being sent upstream to alter the oncoming flow, so that the flow at the obstacle crest remains critical. These upstream disturbances are of the rarefaction type, since their propagation speed decreases as their cumulative amplitude increases. If F_0 lies in the range $0.25 < F_0 < 1$ the upstream propagation speed decreases to zero as H increases, so that the flow becomes critical just upstream; if H is increased further the flow is supercritical over the obstacle, and the upstream flow is not altered. If $F_0 < 0.25$ the lower layer becomes blocked while the upstream flow is still subcritical; further increase in H results in no further change to the upstream flow, because only one layer now flows over the obstacle. The maximum change in the upstream lower layer thickness occurs at $F_0 = 0.25$. This overall picture has been qualitatively verified with experiments for a very similar system in Baines (1984).

3.2. *Three layers*

The corresponding results for a system with three layers are shown in figure 4. The computational procedure for this system is described in I in some detail. There are now two internal wave modes – a fast mode, which for the undisturbed state has the structure of figure 5(*a*), and a slow mode with the structure of figure 5(*b*). As for the two-layer case, for a given value of F_0 there are no upstream disturbances in the

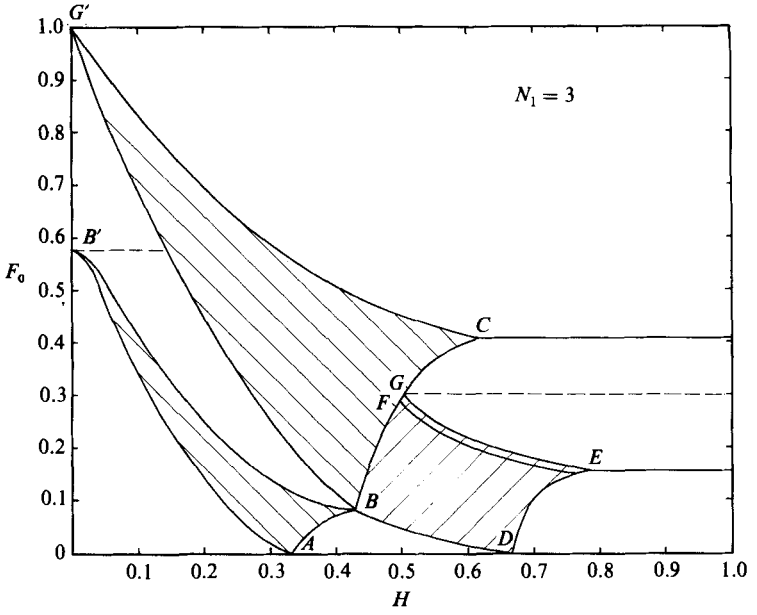

FIGURE 4. (F_0, H)-diagram for three equal layers. The flow is critical at the obstacle crest at the left-hand boundaries of the shaded regions (curves $B'A$, $G'BD$). Layer 1 is blocked to the right of curve ABC, layer 2 to the right of curve DE. Mode 1 is critical upstream to the right of curve GCG'. In the shaded regions, upstream disturbances increase with increasing H. In each unshaded region the upstream flow does not vary with H, as shown in figure 6. N_1 denotes the number of layers.

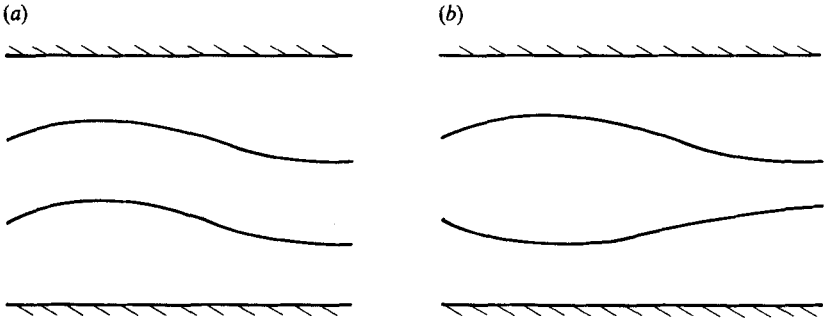

FIGURE 5. The two internal wave modes in the undisturbed three-layer system, represented by positions of the two interfaces: (*a*) fast mode, (*b*) slow mode.

steady state until $H = h_m/D$ is increased to the point where the flow becomes critical at the obstacle crest for the fast mode ($0.575 < F_0 < 1$) or the slow mode ($0 < F_0 < 0.575$), at the boundary of the shaded regions of figure 4. In each case, further increase in the obstacle height results in upstream columnar disturbances of the appropriate mode, to retain critical flow at the obstacle crest (in the shaded regions of figure 4). These upstream disturbances are again of the rarefaction type, with a sign such that the upstream velocity in the lowest layer is always decreased. For $F_0 < 0.575$ this process occurs for increasing H until either the lowest layer becomes blocked ($0 < F_0 < 0.08$ at line AB) or the slow mode becomes critical upstream (at line BB'). When the latter occurs, there is no change in the upstream flow as H increases further until the fast mode becomes critical at the obstacle crest (line BG');

further increases in H then result in upstream rarefactions with the structure of the fast mode until, again, either the lowest layer becomes blocked (line BC) or the flow upstream becomes critical ($c = 0$) with respect to the fast mode (line $G'C$). Of course, the structure of these modes and their propagation speeds vary with the changing mean conditions. Curves of constant velocity and thickness of the bottom layer are shown in figure 6; these show quantitatively the effect of the upstream disturbances on the properties of the lowest layer.

When the lowest layer becomes blocked, only two layers – and hence only one wave mode – pass over the obstacle. As figure 4 implies, this wave mode may be regarded as a form of the fast mode. Upstream, however, disturbances will still propagate on three layers, and hence two modes are still possible. In the shaded region $BDEG$ where the lowest layer is blocked, upstream disturbances must be composed of both modes in such a way as to leave the lowest layer at rest before and after both columnar disturbances have passed. Since the flow is supercritical with respect to the slow mode, the upstream disturbance associated with this mode, at least, must have the form of a jump, and the behaviour of the system is therefore quite complicated. However, as described in I, it is simpler to make the approximation of ignoring the inertia terms in the lowest (stagnant) layer, so that the latter is isostatic: this has the effect of combining the two upstream disturbances so that they may be represented by a single mode. With this approximation and some further modifications as outlined in I, the flow properties of the system when layer 1 is blocked may be obtained. The upstream disturbances then take the form of a jump in region $BDEF$, and a jump plus rarefaction in the region FEG. Similarities between figure 4 and the two-layer diagram figure 3 are evident, with the 'two-layer pattern' appearing three times in figure 4.

Experimental observations of the thickness of the blocked lowest layer in a three-layer system have been made and compared with values computed with the above model. Some examples of these flows are shown in figure 7. The experimental procedure parallels that described in Baines (1984), but with the obstacle towed along the bottom of the 9.17 m long tank. Fluid flow is incident on the obstacle from left to right, and the photographs were taken after the flow reached steady state in the field of view. Mixtures of kerosene and freon were used for the top and bottom layers, with fresh water as the middle layer. Total density variation from top to bottom was approximately 1 ± 0.02 g cm^{-3}. Evaporation of freon from the uppermost layer caused some slight variation in the density of this layer, and $\Delta\rho_1/\Delta\rho_2$ (see I for notation) varied in the range 0.90–1.5. Observations were made with $H = 0.5$ and 0.75, and the results are shown in figure 8. The comparison is generally quite good.

3.3. *Four layers*

The (F_0, H)-diagram for the four-layer system is shown in figure 9. There are now three internal wave modes in the system and, as before, the upstream disturbances are of the rarefaction type for each of these modes, provided that the lowest layer is not blocked. Similarities to the two- and three-layer systems are evident. Apart from the extra mode, before blocking of the lowest layer occurs the four-layer system has the following additional feature. In the range $0.09 < F_0 < 0.15$, the topmost layer (layer 4) becomes 'blocked' whilst the bottom layer (layer 1) still has motion. Since negative fluid velocities upstream may be discounted (they are never observed in experiments unless externally imposed; this is embodied in the computational procedure as assumption A in I), the system must respond to further increases in the obstacle height by generating mode 1 upstream in conjunction with mode 2, at a

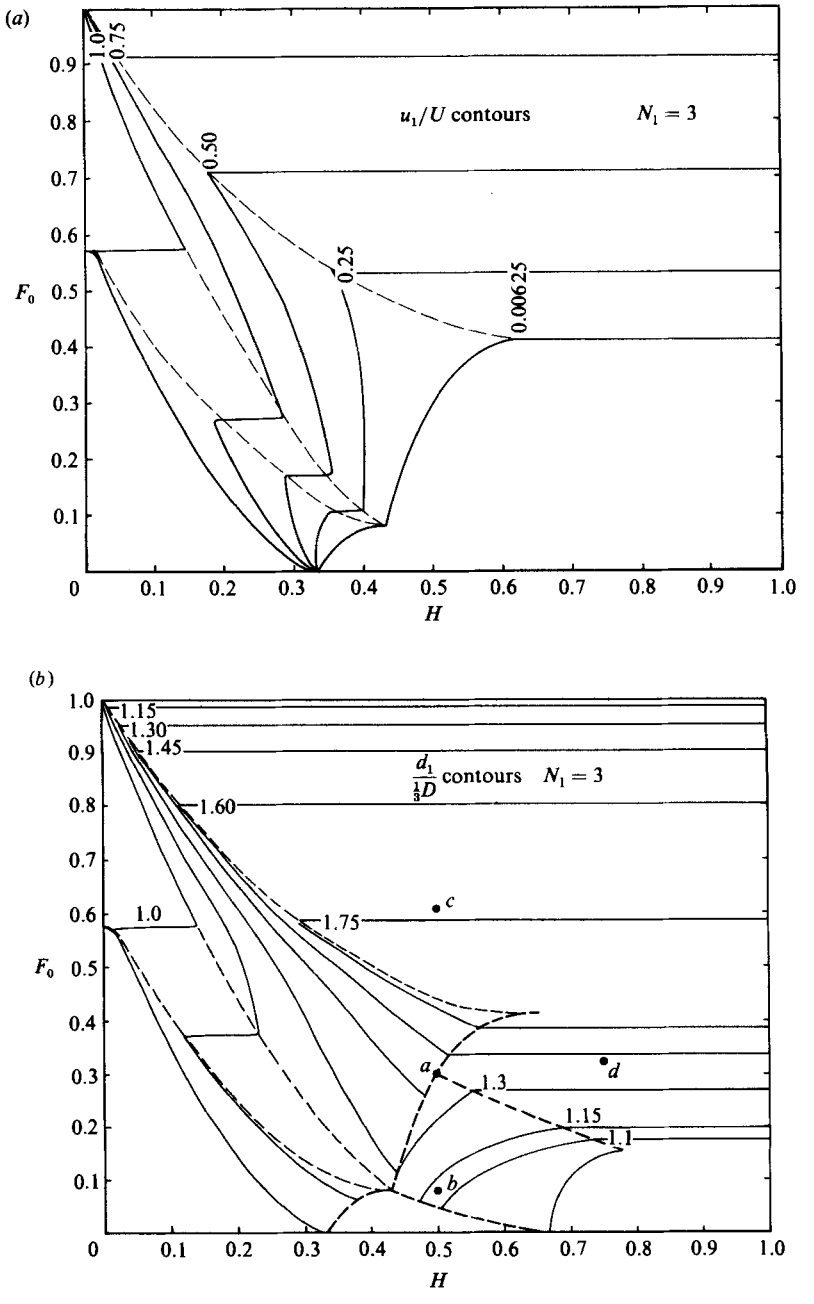

FIGURE 6. For the three-layer system, contours of (*a*) constant upstream velocity u_1 in the lowest layer; the numerical values denote u_1/U. (*b*) constant upstream lowest-layer thickness d_1; the numerical values denote d_1 relative to its undisturbed value, $\frac{1}{3}D$. Dashed lines denote the boundaries of the hatched regions in figure 4. Note that, after it becomes blocked, the lowest layer decreases in thickness as H increases. The points with the letters *a*, *b*, *c* and *d* denote the flow states for the corresponding experiments shown in figure 7.

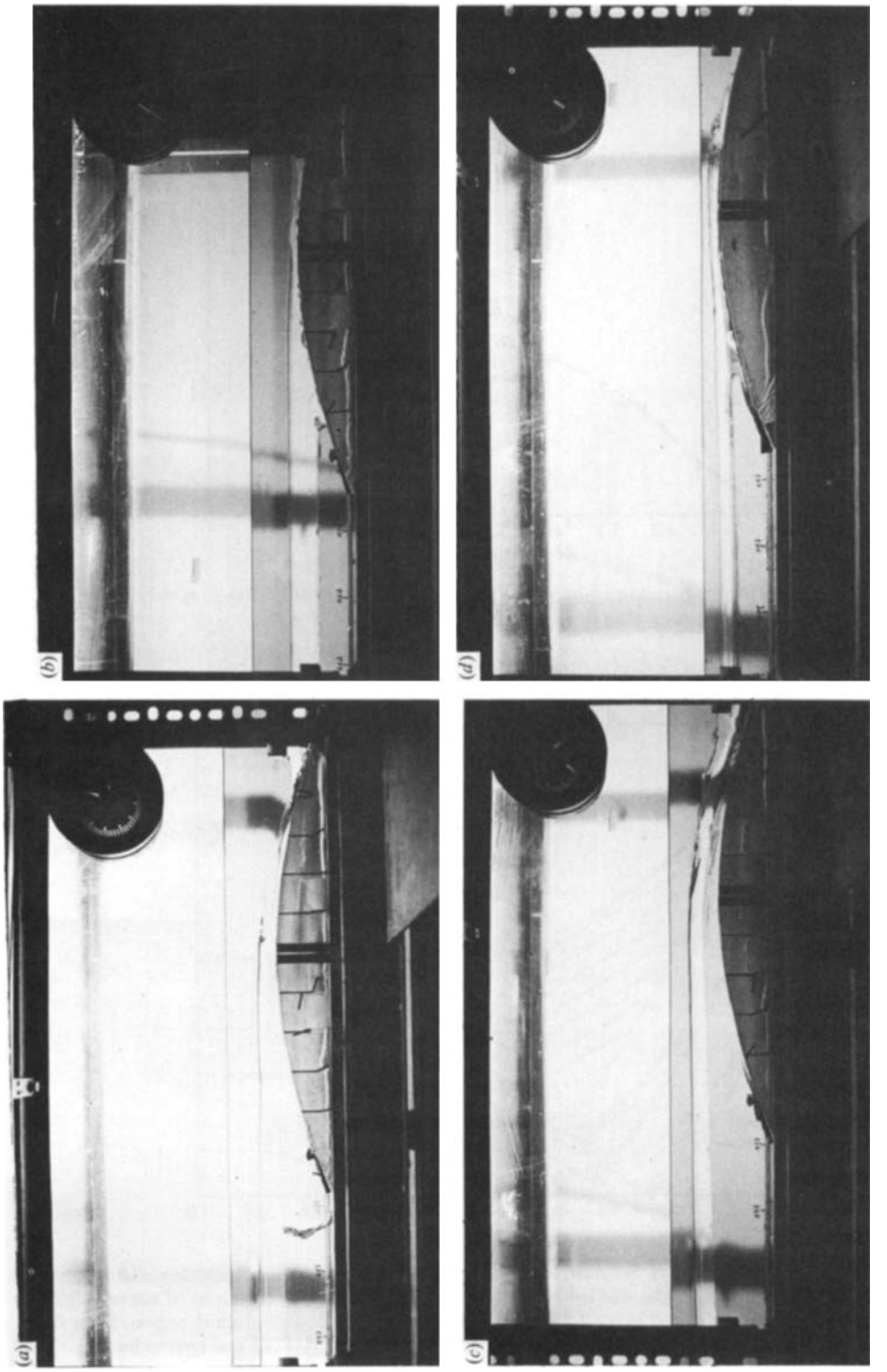

FIGURE 7. Some examples of three-layer flows using water for the middle layer and a mixture of kerosene and freon for the top and bottom layers. The flow is from left to right relative to the obstacle, and has reached a steady state in the field of view. (*a*) $F_0 = 0.3$, $H = 0.5$, (*b*) $F_0 = 0.08$, $H = 0.5$, (*c*) $F_0 = 0.6$, $H = 0.5$, (*d*) $F_0 = 0.32$, $H = 0.75$. The lowest layer is almost blocked in (*b*) and (*d*) and not blocked in (*c*), consistent with figure 4.

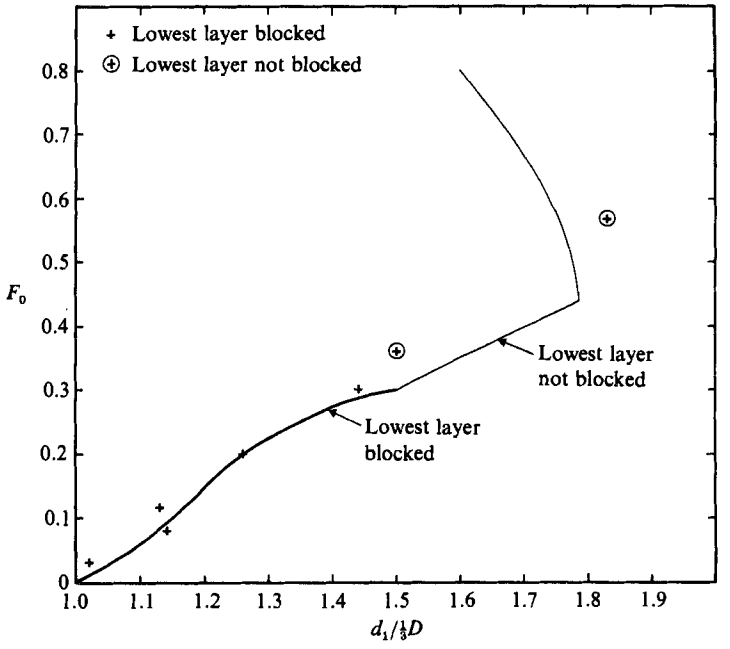

FIGURE 8. Comparison between observed (points) and theoretical values (curve) of the upstream thickness of the lowest layer for $H = 0.5$.

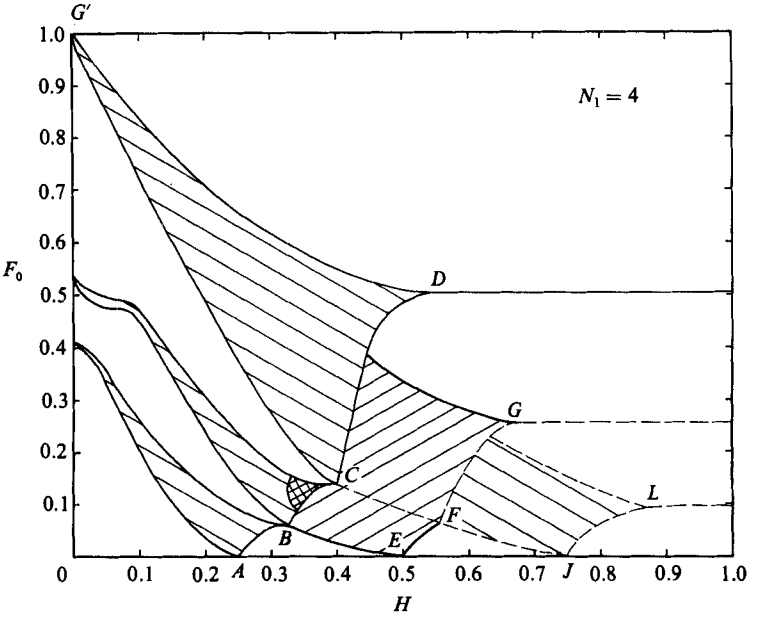

FIGURE 9. The (F_0, H)-diagram for four layers (compare with figure 4). Upstream disturbances increase with increasing H in the shaded regions. Layer 1 is blocked to the right of curve $ABCD$, layer 2 to the right of EFG, and layer 3 to the right of JL. In the double-shaded region, layer 4 is blocked but layer 1 is not. The locations of the boundaries shown dashed are approximate.

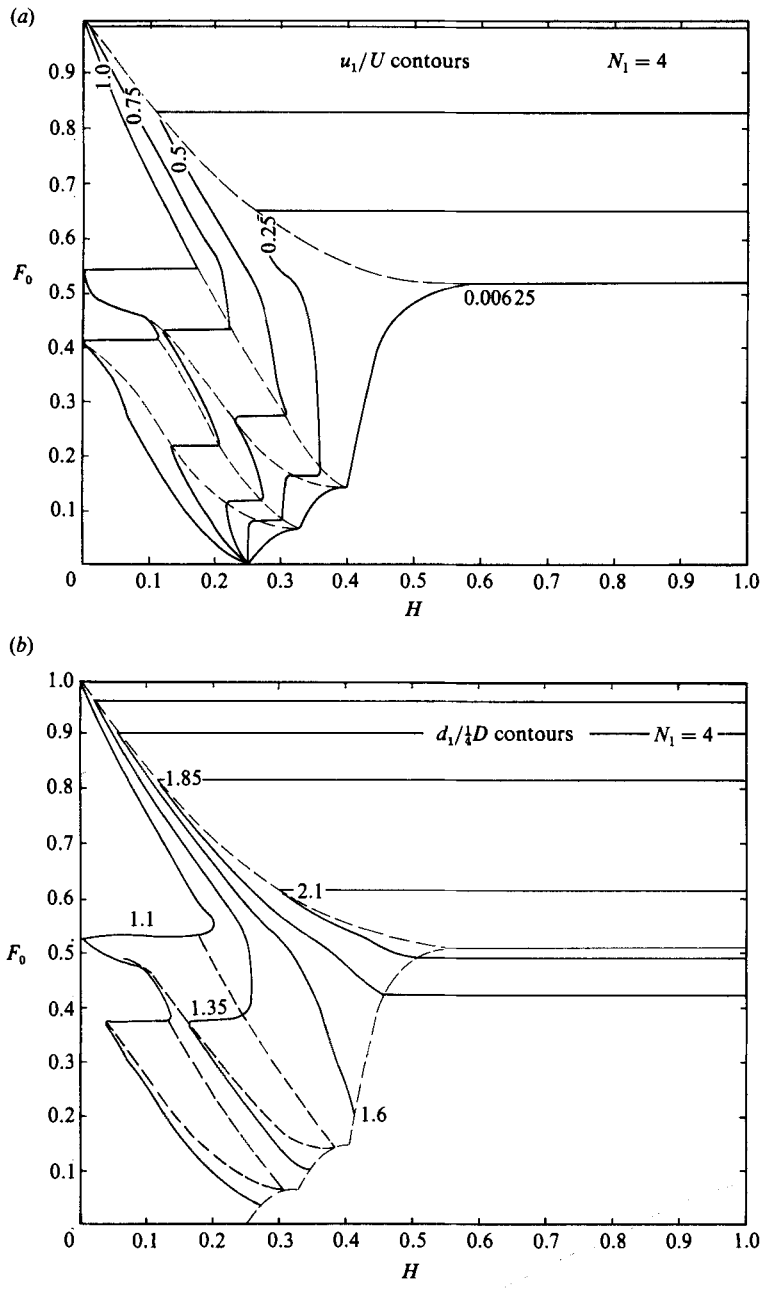

FIGURE 10. For the four-layer system, contours of (*a*) constant upstream velocity u_1 in the lowest layer; the numerical values denote u_1/U. (*b*) constant upstream lowest layer thickness d_1; the numerical values denote d_1 relative to its undisturbed value, $\frac{1}{4}D$. Compare with figure 6 for three layers.

sufficient amplitude to keep layer 4 stationary. This occurs in the double-shaded region of figure 9 and ceases when layer 1 becomes blocked.

Curves of constant velocity and thickness of the bottom layer are shown in figure 10. When the lowest layer became blocked the isostatic-bottom-layer approximation (as used for three-layer systems) was employed, but because of uncertainties in

accuracy some of the boundary curves in figure 9 are shown dashed. The upstream disturbances resulting from further increases in the obstacle height again have the jump or jump-plus-rarefaction form, when either one or two layers are blocked. The form of figure 9 may have been anticipated from the two- and three-layer results, and the increasingly complex patchwork structure of this diagram as the number of layers is increased to five, six or more may be readily envisaged.

4. Nonlinear solutions for sixty-four-layers, as an approximation to continuous stratification

We now describe the application of the general method to a system of sixty-four uniform layers with equal density increments. As before, the layers initially have equal thickness and velocity, so that the system approximates a continuously stratified fluid in uniform motion with constant Brunt–Väisälä frequency N, provided that the overall density variation is small. The speed of the lowest internal wave mode is ND/π, so that $F_0 = U\pi/ND = 1/K$.

From application of the model, the limits of purely sub- and supercritical flow may be obtained. For $F_0 > 1$, the flow is again supercritical everywhere for all obstacle heights and no disturbances are found upstream, whether transient or steady state. For $F_0 < 1$, the numerically determined boundary of subcritical flow for the nth mode is observed to have the equation

$$H = \tfrac{1}{2}(1-nF_0), \quad \frac{1}{n+1} < F_0 < \frac{1}{n}, \quad (n = 1, 2, 3, \ldots). \tag{4.1}$$

This saw-tooth curve (where mode n is critical at the obstacle crest) is shown as the solid line in figure 11, and the line $Nh/U = \frac{1}{2}\pi$ constitutes an envelope for this curve. Only the lowest 5 modes have been studied numerically (i.e. $F_0 > 0.2$) and the extension of this equation to smaller F_0 is due to logical induction. For the layered model the curve must depart from (4.1) as F_0 becomes small. Also shown in figure 11 is the curve for the onset of overturning and enclosed regions ($H = H_s$) obtained from Long's model for continuous stratification, as described in §2. This curve lies to the left of the critical-flow curve (in some regions only slightly), and hence the Long's model solutions without overturning are always subcritical everywhere. In the region where the Long's model solutions are statically stable, comparison between these two solutions shows that they agree reasonably well, e.g. figure 12(*a*). However, they depart significantly as H increases above H_s (the value for overturning for Long's model), even though the layered solution may still be subcritical, e.g. figure 12(*b*). In the Long's model solutions for $2 < K < 3$, etc., where $H_s < H < H_\infty$ the enclosed stagnant regions split the flow into separating streams (e.g. figure 1*b*), in each of which the flow will be supercritical with respect to the relevant mode. In contrast, the layered solutions for these values of H show no 'enclosed regions' or unusual behaviour. For the case of continuous stratification, therefore, it appears that in the parameter range $H_s < H < H_\infty$ where enclosed regions in the Long's model solution occur with $2 < K < 3$, $4 < K < 5$, etc. it appears that two different solutions may be possible if the enclosed regions are interpreted as containing homogeneous stagnant fluid.

As was the case for the number of layers $N_1 = 2$, 3 and 4, when $N_1 = 64$ the upstream disturbances generated when h_m is increased above the critical height have $dc/da \leqslant 0$ (see I for notation), so that the disturbances are of the rarefaction type. As shown in the previous section, if $F_0 > 0.25$ ($N_1 = 2$), 0.42 ($N_1 = 3$) or 0.51 ($N_1 = 4$)

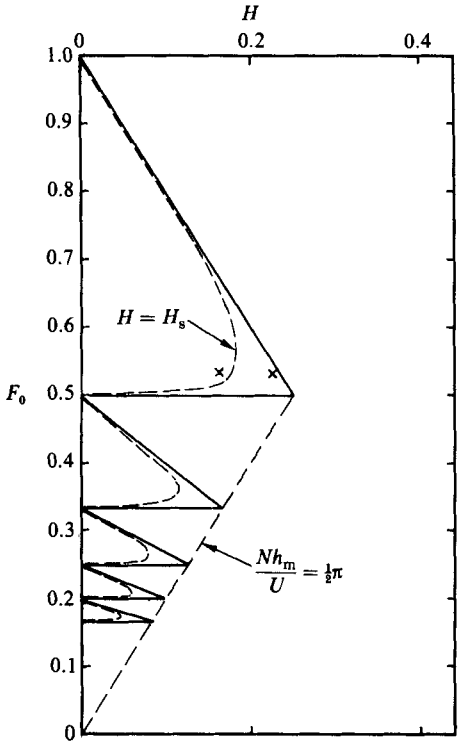

FIGURE 11. The limits of subcritical flow for sixty-four-layers (solid lines). The flow is everywhere subcritical if it is less than the values given by this saw-tooth curve. For these low-order modes the criteria are virtually identical to those for continuous stratification. The curves marking the onset of the enclosed regions in the Long's model solutions (i.e. the curves $H = H_s$ in figure 1) are also shown (dashed lines); for larger H the subcritical layered solutions and the Long's model solutions differ, as shown in figure 12 for the two points denoted by crosses. For $F_0 > 1$, the flow is everywhere supercritical for all H.

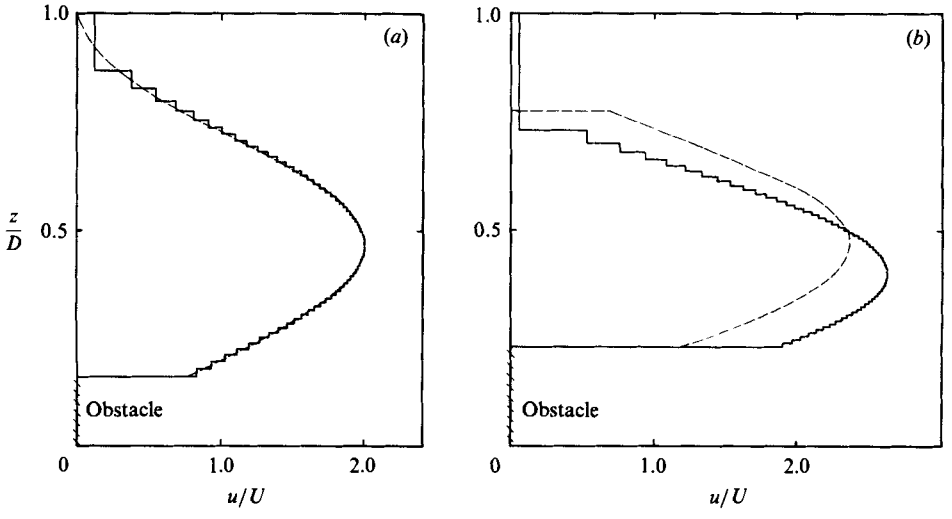

FIGURE 12. Comparison between the velocity profiles at $h = h_m$ for the layered solution and the Long's model solution (shown dashed) for (*a*) $F_0 = 1/K = 0.53$, $H = 0.161$; (*b*) $F_0 = 0.53$, $H = 0.229$. These points are marked by crosses in figure 11.

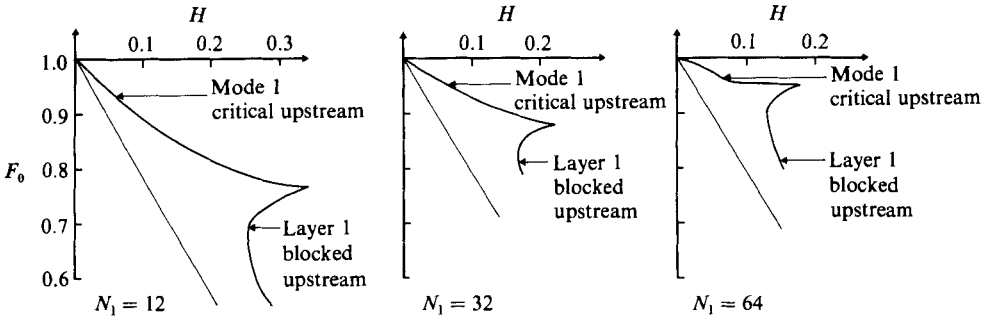

FIGURE 13. The region of (F_0, H)-space where the flow becomes critical upstream with respect to the lowest mode, as a function of the number of layers $N_1 = 12$, 32 and 64. The angled straight lines denote the limit of subcritical flow, as shown in figure 11. Note the similarity to $N_1 = 2$, 3 and 4.

the lowest layer is never blocked for any value of H, and the amplitude of the upstream disturbance is limited by the speed of the fastest mode upstream decreasing to zero. As N_1 increases further this region contracts upwards as shown in figure 13, but even for $N_1 = 64$ it is still significant. The persistence of this phenomenon for large N_1 is at first sight rather surprising, as it implies that the difference between sixty-four-layers and continuous stratification is substantial in the parameter range $0.92 \lesssim F_0 < 1$. The reasons for this are discussed below.

The structure of small-amplitude disturbances in continuously stratified fluid with velocity $U(z)$ and stratification $N(z)$ may be expressed in the form

$$\psi = \epsilon\hat{\psi}(z)\,\mathrm{e}^{\mathrm{i}k(x-ct)}, \tag{4.2}$$

where $\hat{\psi}(z)$ is governed by the Taylor–Goldstein equation

$$\frac{\mathrm{d}^2\hat{\psi}}{\mathrm{d}z^2} + \left(\frac{N^2}{(U-c)^2} - \frac{\mathrm{d}^2U/\mathrm{d}z^2}{U-c}\right)\hat{\psi} = 0, \tag{4.3}$$

with

$$\hat{\psi} = 0 \quad \text{at } z = 0, D,$$

where the wave speed c is an eigenvalue. If the disturbance takes the form of a columnar disturbance mode of amplitude ϵ, the resulting horizontal velocity and density profiles are

$$u = U_0(z) - \epsilon\frac{\mathrm{d}\hat{\psi}}{\mathrm{d}z},$$

$$\rho = \rho_0(z) - \epsilon\frac{\mathrm{d}\rho_0}{\mathrm{d}z}\frac{\hat{\psi}(z)}{U_0-c} + O(\epsilon^2), \tag{4.4}$$

where the subscript zero denotes initial values. If the values U_0 and N_0 are constant, as is the case for the flows under discussion here, then (4.3) has the solutions

$$\hat{\psi} = \sin\frac{n\pi z}{D}, \quad c = c_n = -U_0\left(\frac{K}{n} - 1\right) \quad (n = 1, 2, 3, \ldots), \tag{4.5}$$

where, as in §2, $K = ND/\pi U_0$. If (4.4) for some specific mode m is substituted into (4.3) and the resulting profiles used for U, N in (4.3), then (4.5) is again a solution provided $n = m$, with error of $O(\epsilon^2)$. This implies that $\mathrm{d}c/\mathrm{d}a$ (see I) is zero when U and N are constant, and that the structure of the eigenfunction also does not change with amplitude initially. In fact, from the numerical computations the structure of the

velocity profile remains sinusoidal to a very good approximation for quite large amplitudes as H increases; also, the eigenvalues decrease slowly except when $F_0 > 0.95$, where the initial decrease is slow but subsequently becomes more rapid until $c = 0$.

Internal wave modes $n \neq m$ (the mode of the existing upstream columnar disturbance) are affected much more substantially as columnar mode m increases in amplitude – the modal structure becomes progressively more non-sinusoidal, and the speed of propagation may vary significantly. In particular, for $0.5 < F_0 < 0.95$, as the amplitude of the columnar mode 1 upstream increases, the speed c_2 of the second mode (which is initially positive, i.e. directed downstream) decreases to zero and then becomes negative. However, if columnar mode 2 is introduced upstream, this has the effect of increasing the speed c_2 (in the downstream direction). In the present circumstances, the equations for steady-state flow show that a finite negative value for c_2 is not possible (as this would imply critical flow for mode 2 on the forward-face of the obstacle), so that the amplitude of mode 2 upstream must be adjusted so that $c_2 = 0$ there. Consequently, as H increases, both modes 1 and 2 increase upstream, with $c_2 = 0$ upstream and $c_1 = 0$ at the obstacle crest, until the lowest layer becomes blocked. The program based on the general method described in I achieves this by alternating between the two modes for the upstream disturbance, depending on which mode has the smallest negative eigenvalue. The locations in terms of F_0, H where mode 2 first appears and where the lowest layer becomes blocked are indicated in figure 14, which displays the main results of this paper. Note that the upstream disturbance increases rapidly with H, ranging from zero (where the flow first becomes critical at the obstacle crest) to 'unity' (blocked flow) over a typical range of H of 0.05.

For $\frac{1}{3} < F_0 < \frac{1}{2}$, as H increases above the critical height the mode generated upstream is mode 2. For $0.46 < F_0 < 0.5$, as H and the upstream amplitude of mode 2 increase, c_2 eventually increases to zero; further increase in H then causes no change in the upstream motion until mode 1 becomes critical at $\mathrm{d}h/\mathrm{d}x = 0$. On the (F_0, H)-diagram, this occurs at a continuation of the curve for mode 1 critical for $F_0 > 0.5$. This behaviour parallels that of mode 1 in the range $0.95 < F_0 < 1$, and it is found again for mode 3 in the range $0.31 < F_0 < 0.333$. For $0.31 < F_0 < 0.46$, c_2 does not become zero, and the motion is governed by modes 2 and 3, in a manner paralleling that for modes 1 and 2 for $0.46 < F_0 < 0.9$. Similar behaviour occurs with modes 3 and 4 when $F_0 < 0.31$.

Comparisons have been made between these results for $N_1 = 64$ and some corresponding results for $N_1 = 128$. Over most of the range of F_0 the comparison is quite good. One systematic difference exists, however: the region of upstream critical flow for $0.95 < F_0 < 1$ for $N_1 = 64$ is reduced for $N_1 = 128$, continuing the trend shown in figure 13, and similar reductions were also found in the corresponding regions for modes 2 ($0.46 < F_0 < 0.5$) and 3 ($0.31 < F_0 < 0.333$). One therefore expects these ranges to shrink to zero as N_1 tends to infinity. We may infer that sixty-four-layers is not a good approximation to continuous stratification if F_0 lies in these ranges but it should be satisfactory elsewhere, at least up to the point of blocking.

Also shown in figure 14 is the line $Nh_m/U = 2$. We note that this acts as an envelope for the blocking curve, and almost coincides with it in many places. This is consistent with the experimental results of the author (Baines 1979*b*) where upstream blocking (albeit for short obstacles) was observed to occur in initially uniform stratification for $Nh_m/U \gtrsim 2$ when $F_0 \lesssim 0.5$.

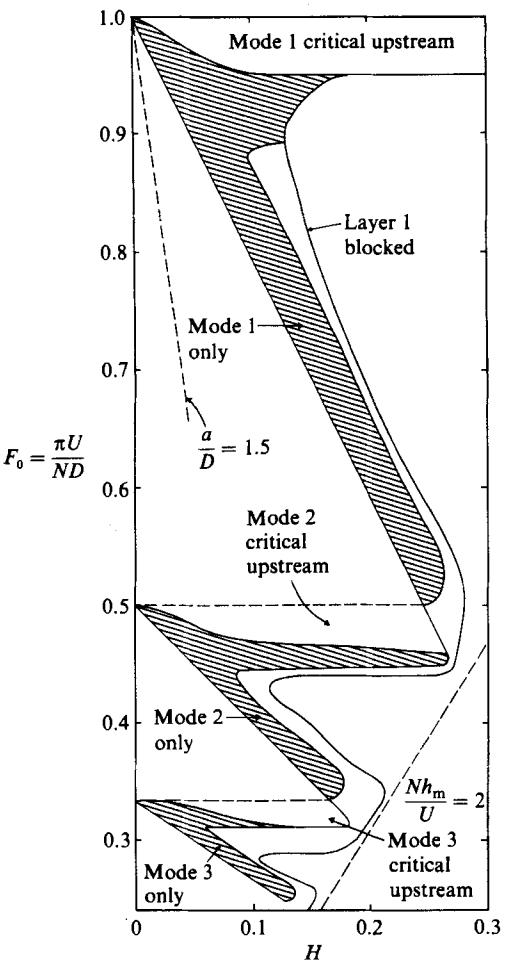

FIGURE 14. The (F_0, H)-diagram for $N_1 = 64$, showing the limit of subcritical flow (as in figure 11), the regions (hatched) where the upstream disturbance consists of a single mode, and the curve marking the onset of blocking of the lowest layer. For $F_0 < 0.4$ the blocking curve is approximate, due to scatter in the numerical results. The dashed line (bottom right) denotes $Nh_m/U = 2$. The line marked $a/D \approx 1.5$ denotes the onset of upstream disturbances from experiments in uniformly stratified fluid (Baines 1979*a*) with this approximate value of a/D.

The numerical results for $F_0 < 0.3$ are reasonably consistent but show some scatter when the upstream disturbance is composed of more than one mode. This is due to the fact that a very small eigenvalue is usually present which may be positive or negative, and the computational procedure is sensitive to this. This constitutes a limitation on the procedure in its present form.

Upstream velocity profiles at the point of blocking of the lowest layer are shown in figure 15 for a range of values of F_0, together with a representative profile for the range $0.95 < F_0 < 1$ ($F_0 = 0.98$) showing the maximum disturbance upstream. The changing dominant modal structure with F_0 is evident in these profiles. It is also clear that the reason why sixty-four layers do not always represent continuous stratification adequately is because the slow-moving layers become very broad when the upstream disturbance becomes large, so that their discrete nature becomes much more significant. Consequently, the departure from the dynamical properties of a

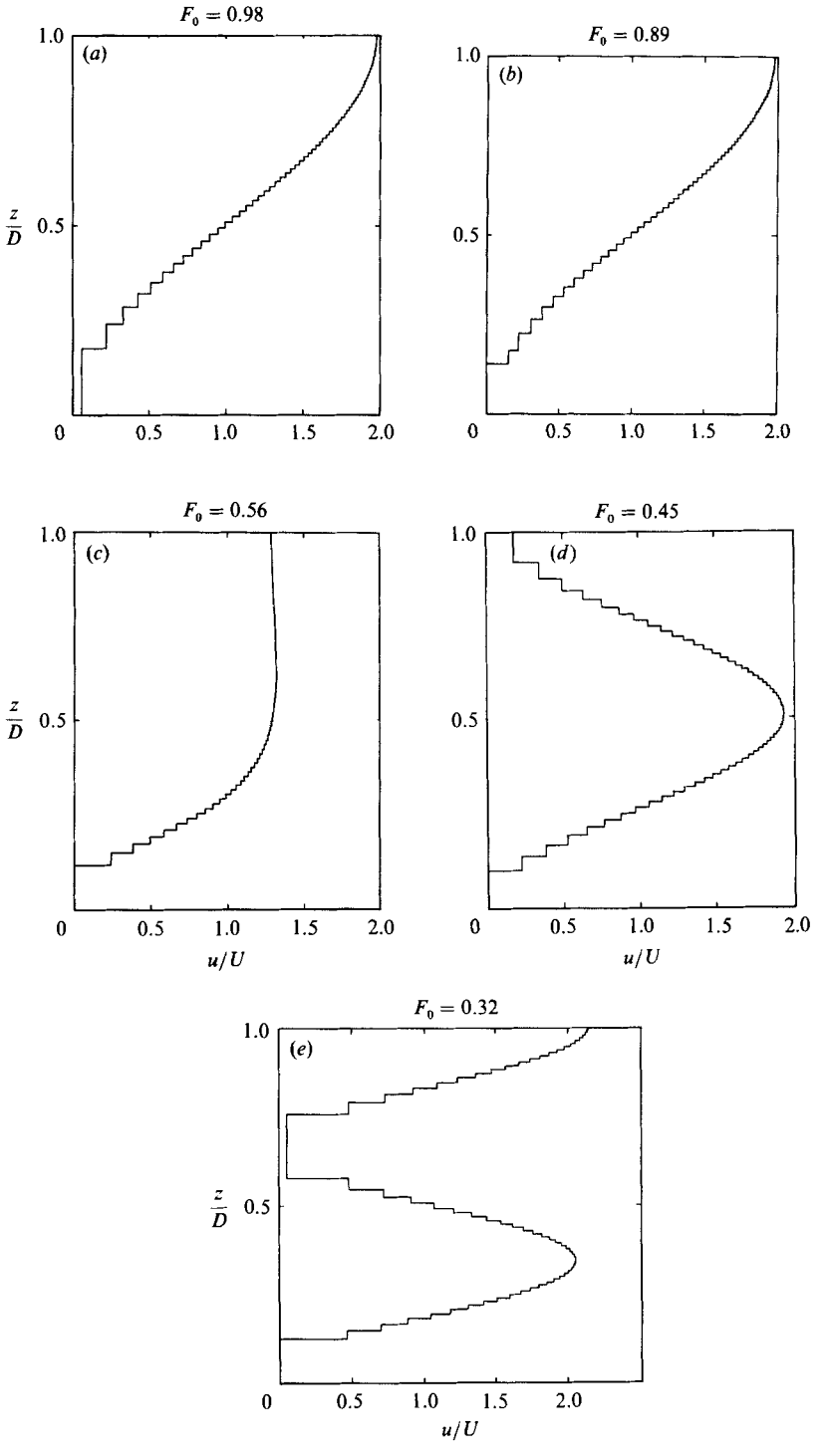

FIGURE 15. Some representative upstream velocity profiles for the sixty-four-layer model. (*a*) at the point of maximum upstream disturbance for $F_0 = 0.98$ (i.e. $H \geqslant 0$); at the point of blocking for (*b*) $F_0 = 0.89$, (*c*) $F_0 = 0.56$, (*d*) $F_0 = 0.45$, (*e*) $F_0 = 0.32$.

continuous profile is hardly surprising, and from figure 14 we might expect the system to behave like a system with a smaller total number of layers as the disturbance amplitude increases.

5. The phenomenon of blocking

The nature of upstream blocking in stratified fluids has been obscure until recently. We now know that, in large-Reynolds-number flows, upstream blocking is a wave phenomenon due to propagating columnar disturbance modes which may have jump or rarefaction character. In the layered systems described in this paper, the following characteristics of the formation of an upstream-blocked lowest layer may be noted.

As the thickness of the lowest layer decreases to zero at the obstacle crest with increasing obstacle height, the speeds of one internal wave mode (directed both upstream and downstream) converge to the speed of the fluid in this thinning layer;† this mode then disappears when the layer is no longer present. Decreasing lowest-layer velocity upstream implies decreasing transport and decreasing thickness of this layer over the obstacle, but the fluid velocity at the obstacle crest may still be finite as the layer thickness vanishes. An exception to this is the range of the smallest values of F_0, where the upstream disturbance causing blocking consists only of the highest (slowest) mode (this happens for $N_1 = 2$, 3 and 4 but may not apply to $N_1 = 64$). At the obstacle crest it is this mode which is critical, and it is this mode which must also vanish as the lowest layer disappears. Hence, as the lowest-layer thickness approaches zero at the crest, under these circumstances the fluid speed there must also vanish. Applying Bernoulli's equation to the lowest layer when the velocity is small then suggests that, at the point of blocking, the depth of the layer upstream is equal to the height of the obstacle. This is in fact the case for $N_1 = 2$, 3, and 4, for the appropriate ranges of F_0.

For larger values of F_0, the depth of the blocked layer at the point of blocking d_b increases with F_0 from a value somewhat less than h_m to a value equal to or slightly greater than h_m, over the range of dominance of each particular mode. The values of d_b/h_m for three, four and sixty-four-layers are shown in figure 16. In the range studied, for $N_1 = 64$, d_b/h_m varies between 0.5 and 1. The computed results for $N_1 = 64$ show some scatter due to the nature of the numerical procedure, and the curves presented are mean values. In fact, the depth of the blocked layer for $N_1 = 64$ is remarkably independent of h_m over the range investigated ($F_0 > 0.23$), and most numerical values satisfy

$$d_b/D = 0.12 \pm 0.02,$$

with a slight upward trend with F_0. Another point of interest is the mean density gradient in the blocked fluid; at the point of blocking in these layered models this gradient will be zero, but it will increase as the obstacle height increases and higher layers also become blocked. It is difficult to draw general inferences from the three- and four-layer results, but it is obvious that the blocked fluid will always be much more weakly stratified than the initial undisturbed fluid.

† In fact, as may be seen from (3.8) of I, if the thickness of any fluid layer becomes vanishingly small, the two wave speeds of one mode converge to the fluid speed of that layer, and this mode vanishes if the layer vanishes.

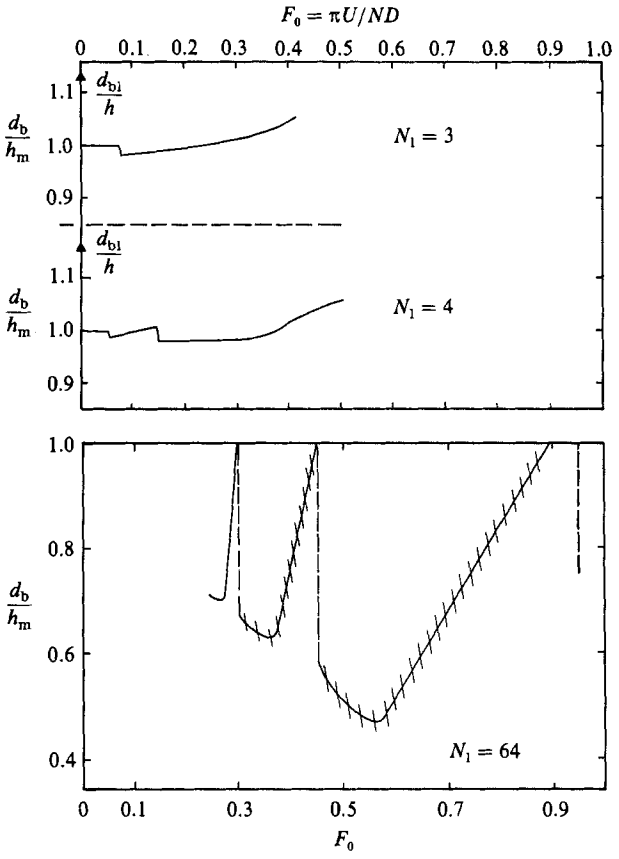

FIGURE 16. Depth of the blocked bottom layer d_b at the point of blocking, relative to h_m as a function of F_0 for three, four and sixty-four-layers. In the hatched regions the curve is approximate as there is some scatter in the numerical results. The vertical dashed lines when $N_1 = 64$ correspond to the F_0 values where the 'layer 1 blocked' curve of figure 14 is nearly horizontal, implying a change in the dominant mode.

6. Summary and discussion

We have examined the flow of a system of homogeneous fluid layers of finite depth over long obstacles with the hydrostatic approximation, using the model and procedure described in Baines (1988). The study may be seen as a contribution to stratified hydraulics. The resulting flows have been calculated as initial-value problems, with the obstacle introduced into fluid in which the velocity is initially uniform with height and the layers have equal thickness and equal density increments. The results from these calculations may be summarized as follows. There are no upstream disturbances in the resulting flow if $F_0 > 1$, and the steady-state flow is everywhere supercritical. For $F_0 < 1$ the upstream disturbances initially have the form of rarefactions, regardless of the number of (equal) layers. For two fluid layers the results are relatively simple and are virtually the same as those described in Baines (1984) for a slightly different system: as the obstacle height increases, for $F_0 < 0.25$ the lower layer eventually becomes blocked, but for $0.25 < F_0 < 1$ the upstream flow eventually becomes critical and the disturbance reaches a maximum amplitude which does not block the lower layer. For the three-layer system,

upstream blocking of the lowest layer may be achieved if $F_0 < 0.41$, and for the middle layer if $F_0 < 0.3$. Laboratory experiments illustrating blocking in three-layer flows are consistent with these results. For four layers, the lowest layer may become blocked if $F_0 < 0.52$, the second if $F_0 < 0.145$ and the third if $F_0 < 0.065$, if H is sufficiently large. The four-layer system has the surprising property that, over a significant range of values of F_0 and H, layer 4 (the uppermost) is blocked upstream (i.e. is stagnant) but layers 1, 2 and 3 are not.

The sixty-four-layer model is intended as an approximation to continuous stratification. In the range investigated, $0.2 < F_0 < 1$, the approximation is quite good provided that the upstream disturbances are small. As they increase in amplitude the slower-moving layers become much thicker, and this causes the velocity and density profiles to depart substantially from those of a continuous stratification, even if only one mode is present upstream. Once the flow becomes critical at the obstacle crest, the rate of increase in amplitude of the upstream disturbance is very rapid, in that a relatively small change in H (say 0.05) can result in the upstream disturbance increasing from zero to unity (implying blocked fluid). For $0.95 < F_0 < 1$, however, the blocking does not occur owing to the finite number of layers, and the flow becomes critical upstream in the same manner as for two, three or four layers. This behaviour also occurs for higher modes at lower F_0, and suggests that the representation of continuous stratification by such a layered system may be imperfect for large-amplitude disturbances over a range of F_0 which is just subcritical for each mode.

Some laboratory experiments with towed obstacles and continuously stratified fluid with constant N were carried out to investigate the general relevance of the present results. The procedure and techniques were the same as those described in Baines (1979*a*,*b*). In experiments of this nature, hydrostatic flow is only achieved with very long obstacles, namely those with lengths much greater than the channel depth. Such long obstacles result in long upstream transients which take a long time to leave the vicinity of the obstacle. Separating the transient from the steady-state upstream phenomena is consequently much more difficult than for shorter obstacles, and the tank used is not sufficiently long to permit this separation, if the obstacles are long enough to guarantee hydrostatic flow. Hence the obstacles used in these experiments were somewhat shorter, so that a quantitative comparison between the observations and the hydrostatic theory is not warranted. However, the flows were more nearly hydrostatic than those studied in Baines (1979*a*) in that a/D was larger (a is the obstacle half-length), and the upstream amplitudes were observed to be substantially closer to those predicted by the present model. It is generally observed that, for uniform velocity and stratification, upstream disturbances appear for smaller obstacle heights in non-hydrostatic flows than for hydrostatic ones.

We have investigated the relationship between the present solutions with layered models and the Long's model solutions with continuous stratification, for the same values of F_0 and H. These solutions appear to agree quite well when F_0 and H are such that the Long's model solutions are statically stable, but they differ substantially when the latter are unstable and closed flow regions occur. Such enclosed regions do not arise in the layered solutions. In the non-hydrostatic laboratory experiments, the large-amplitude Long's model solutions *per se* have not been observed, although closed stagnant regions are common when the obstacle is sufficiently large. The reason for this may be that the flows are difficult to set up; they may also be unstable since, as Long (1955) showed, $Ri < \frac{1}{4}$ in these flows even before stagnant regions are established.

A significant result of this study is the corroboration from the sixty-four-layer results that the criterion for blocking in uniformly stratified flow is $Nh/U \gtrsim 2$, provided two or more modes are present. This criterion seems to be much less sensitive to the modal structure than that for the onset of the upstream disturbances, which has a saw-tooth pattern on the (F_0, H)-diagram.

The authors are most grateful to Julie Golds, who played a substantial part in the development of the numerical model in the early stages of this work, to David Murray for assistance with the experiments, and to Carol Drew for typing the manuscript.

REFERENCES

BAINES, P. G. 1977 Upstream influence and Long's model in stratified flows. *J. Fluid Mech.* **82**, 147–159.

BAINES, P. G. 1979*a* Observations of stratified flow over two-dimensional obstacles in fluid of finite depth. *Tellus* **31**, 351–371.

BAINES, P. G. 1979*b* Observations of stratified flow part three-dimensional barriers. *J. Geophys. Res.* **83**, 7834–7838.

BAINES, P. G. 1984 A unified description of two-layer flow over topography. *J. Fluid Mech.* **146**, 127–167.

BAINES, P. G. 1988 A general method for determining upstream effects in stratified flow of finite depth over two-dimensional obstacles. *J. Fluid Mech.* **188**, 1–22.

GRIMSHAW, R. H. J. & N. SMYTH 1986 Resonant flow of a stratified fluid over topography. *J. Fluid Mech.* **169**, 429–464.

LONG, R. R. 1955 Some aspects of the flow of stratified fluid, III. Continuous density gradients. *Tellus* **7**, 341–357.

MCINTYRE, M. E. 1972 On Long's hypothesis of no upstream influence in uniformly stratified or rotating flow. *J. Fluid Mech.* **52**, 209–243.

MELVILLE, W. K. & HELFRICH, K. R. 1987 Transcritical two-layer flow over topography. *J. Fluid Mech.* **178**, 31–52.

WEI, S. W., KAO, T. W. & PAO, H.-P. 1975 Experimental study of upstream influence in the two-dimensional flow of a stratified fluid over an obstacle. *Geophys. Fluid Dyn.* **6**, 315–336.

WONG, K. K. & KAO, T. W. 1970 Stratified flow over extended obstacles and its application to topographical effect on ambient wind shear. *J. Atmos. Sci.* **27**, 884–889.